Earth Reinforcement, Ochiai, Yasufuku & Omine (eds) © 1996 Balkema, Rotterdam. ISBN 90 5410 833 9

Behavior of reinforced earth embankments on liquefiable sandy ground

R. Uzuoka & M. Mihara
Hazama Corporation, Tokyo, Japan
F. Oka & A. Yashima
Gifu University, Japan

ABSTRACT: Dynamic response of a reinforced embankment on liquefiable ground and the effectiveness of reinforcement in preventing a large deformation was investigated. In this study, a numerical simulation of liquefaction was carried out using an effective stress analysis, based on data from shaking table tests of a reinforced embankment using non-woven fabric on liquefiable ground. It was found that: 1) The effectiveness of reinforcement using non-woven fabric on the reduction in embankment subsidence is small. 2) Reinforcement using non-woven fabric can control the occurrence of tensile stress in the embankment to a certain degree, but further study is required in regard to the effectiveness of reinforcement in preventing the failure of the embankment. 3) Reinforcing the embankment into a single body would be effective in reducing the embankment subsidence.

1 INTRODUCTION

Reinforced-earth methods using materials such as geotextiles and geogrids have been recently used at many sites. A number of major earthquakes have taken place in recent years, and there is now heightened interest in the behavior of reinforced-earth structures during earthquakes. The Great Hanshin-Awaji Earthquake led to a confirmation of the earthquake-resistance of reinforced-earth retaining walls used at railway slopes (Tatsuoka 1995). There have also been reported that damages caused to reinforced-earth structures such as embankments and retaining walls by the Northridge Earthquake was light (White et al. 1994).

Earth-reinforcement is sometimes used to bundle an embankment into a single body on a soft clay ground, thereby controlling deformation due to lateral flow in the ground, and to additionally control the failure of the embankment itself. When an earthquake strikes and the foundation ground liquefies, the behavior of the embankment on a liquefied ground is thought to be similar to the behavior of an embankment on a soft clay ground — and the amount of deformation of an embankment on liquefiable ground can be controlled by reinforced-earth methods. As the earth-reinforcing deals only with the embankment itself, it cannot be expected to have a significant effect in preventing the liquefaction of the foundation ground. Although the earth-reinforcing allows the embankment subsidence, the extensive deformation of the embankment could be avoided. The retaining its function of the embankment as a structure and easy restoration are thought to be important in terms of the ductility of the structure (Fukuda 1991).

Few studies have been carried out in regard to the seismic behavior of reinforced-earth embankments on sandy ground that may liquefy during an earthquake. The Public Works Research Institute (PWRI 1989) has studied the behavior of reinforced embankments on saturated sandy ground using large-scale shaking tables.

In this study, the numerical simulations of liquefaction were carried out — using effective stress analysis and based on data from a shaking table test of a model reinforced embankment on liquefiable ground, carried out by PWRI — in order to study the dynamic response of reinforced embankments on liquefiable ground, and the effectiveness of reinforced-earth methods in controlling the deformation of embankments.

2 SHAKING TABLE TEST

The shaking table test investigated in this study was carried out by the Public Works Research Institute of the Ministry of Construction in order to study the effectiveness of reinforced-earth methods in controlling the subsidence and deformation of embankments on a liquefiable ground.

2.1 *Testing method*

Shaking table tests were carried out for four differently

reinforced models. The different test cases are shown in Table 1. In this study, we picked up the result of only Model 1 using non-woven fabric as the reinforcement. The section of the models is shown in Figure 1. A steel casing 8 m long in the direction of shaking, 2 m high, and 1 m deep was used. Two unsaturated embankments were constructed on top the saturated sandy ground with 1.3 m thickness. This model had the reinforcement with five layers of non-woven fabric. The non-woven fabric consisted of 70% nylon and 30% polyester, and was 0.217 mm thick. Sengenyama sand was used for both embankments and foundation grounds. The model was constructed by laying a certain thickness of sand, treading the surface to get a relative density of 50% and then saturating. In order to reduce the reflected input wave from the side walls, urethane foam was placed between the side of the ground and the casing wall.

Measurements of the acceleration in the ground and the embankments, the pore water pressure in the ground, the vertical displacement at the embankment crest and at the ground surface, and the tensile stress of the reinforcing material were made. The velocity of secondary waves were also measured before the shaking.

Test results will be summarized analytical results.

Table 1. Test cases

Model No.	Reinforcement method	
	Left embankment	Rightembankment
1	Non-woven fabric (5layers)	-
2	Non-woven fabric (5layers)	-
	Compacted underneath the embankments	
3	Net (1layer) with soilbag	Net (5 layers) with soilbag
4	10 Reinforcing bars (1 layer) Non-woven fabric (1 layer)	50 Reinforcing bars (5 layers) Non-woven fabric (1 layer)

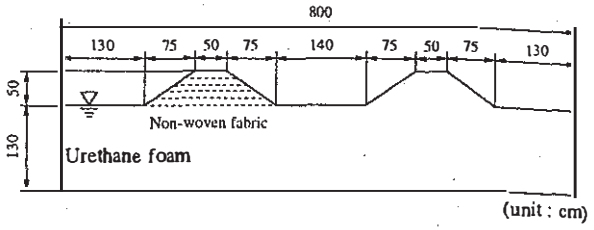

Figure 1. Section of the model

3 EFFECTIVE STRESS ANALYSIS

3.1 *Analytical method*

LIQCA (Shibata et al. 1991), effective stress based numerical analysis program which incorporates a cyclic elastoplastic model of sand was used for the analysis of liquefaction. The governing equations for LIQCA are based on a u-p (displacement of solid phase-pore water pressure) formulation which combines an equilibrium equation and a continuity equation. The finite element method was used for space discretization for the equilibrium equation , and the finite difference method was used for the continuity equation. The Newmark's β method was used for the time integration.

The constitutive equation used for the sand was a cyclic elastoplastic model (Oka et al. 1994). This constitutive equation is formulated based on the concepts of infinitesimal strain, non-associated flow rule, non-linear kinematic hardening rule, and the overconsolidation boundary surface. In order to improve the behavior after the effective stress reaching the phase transformation line , the constitutive equation used in this study reduces the elastic shear modulus G_E after the stress reaching the phase transformation line using the following equation (Tateishi et al. 1995).

$$G_E' = \frac{G_E}{1 + \gamma^p / \gamma_r^p} \tag{1}$$

where γ^p is the invariant of the deviatric plastic strain and γ_r^p is the parameter. From Equation (1), the hysteresis damping after phase transformation line increases, and a smoother hysteresis curve is obtained. In order to express the fading memory for an anisotropically consolidated sand, the invariant of the initial stress ratio η_0 which control the dilatancy behavior was reduced using the following equation (Tateishi et al. 1995).

$$\eta_0' = \exp(-C_d \gamma^p)\, \eta_0 \tag{2}$$

where C_d is the parameter.

3.2 *Analytical conditions*

The cyclic elastoplastic model for sand mentioned above was used for the saturated sandy ground and the embankments. Numerical constants used were obtained from measurements taken during the fabrication of the test models, and from existing data derived from past tests. The parameters for Equations 1 and 2 were determined by trial and error, through simulations of element tests carried out to get the required liquefaction strength. The liquefaction strength has been obtained from cyclic torsional shear tests of Sengenyama sand with a relative density of 50% (Tatsuoka 1982). As an example of simulation of element tests, the stress-strain relationship and the effective stress path with 10 cycles, are shown in Figure 2. Table 2 shows the model parameters of the saturated ground and the embankments.

The non-woven fabric was modeled as beam elements with low rigidity. Slippage between the non-woven fabric and the embankment material was not taken into account. The parameters for the beam elements was determined mainly from plane-strain tension tests (Tatsuoka 1986). Table 3 shows the model

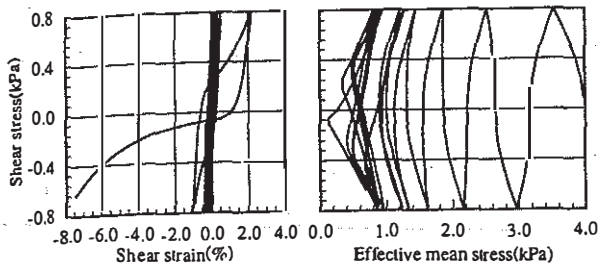

Figure 2. An example of simulation results from element tests

Table 2. Model parameters of the saturated ground and the embankment.

		Dr=50% embankment	Dr=50% ground
Density	ρ	1.585 t/m³	1.937 t/m³
Initial void ratio	e_0	0.837	0.837
Coefficient of permeability	k	-	8.0E-5 m/s
Compression index	λ	5.00E-3	5.00E-3
Swelling index	κ	2.25E-4	2.83E-4
Initial Shear modulus	G_0	15850 kPa	19370 kPa
Poisson's ratio	ν	0.2	0.2
Failure stress ratio	M_f	0.909	0.909
Phase transformation stress ratio	M_m	1.105	1.105
Overconsolidation ratio	OCR	1.2	1.2
Control parameter of anisotropy	C_d	2000	2000
Reference strain	γ_r	0.002	0.002

Table 3. Model parameters of the non-woven fabric

Elastic modulus	E	9800 kPa
Density	ρ	1.00E-6
Cross-sectional area	A	2.17E-4 m²

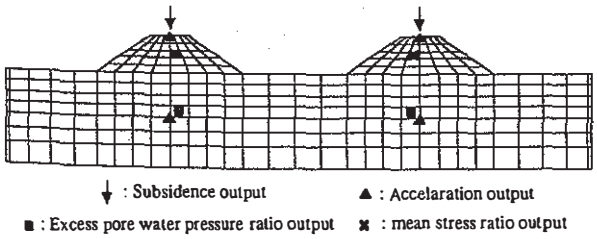

Figure 3. Analytical model

parameters of the non-woven fabric.

The analysis was carried on model scale. Figure 3 shows the analytical model. In the model the urethane foam between the side of the ground and the casing wall was considered. In figure 3, output points of nodes and elements are shown. The time-step increment was selected as 0.01 second. Rayleigh's damping — damping proportional to rigidity — was used as viscous damping. The damping coefficient was set at 0.001, assuming that damping is 5%. The input motion was 40 sinusoidal waves of a frequency of 2 Hz, producing a maximum acceleration of 173 gal. The duration of the analysis was 20 seconds.

4 ANALYTICAL RESULTS

4.1 *Comparison with Total Stress Analysis (Analytical Case 1)*

Permanent deformation analysis was also carried for Model 1 by the total stress analysis (The Public Works Research Institute et al. 1996). In this analysis method, the relationship between stress and strain after liquefaction is estimated from the dynamic total stress response analysis, and the static stress state obtained from initial stress analysis (Koseki et al. 1995). The parameters for the analytical model in this permanent deformation analysis were also determined from the measurement results from the model fabrication and existing data from laboratory tests.

The results of the total stress analysis and effective stress analysis for the tests on Model 1 are discussed together.

(1) Acceleration response

Table 4 summarizes the peak acceleration and amplification ratio to the input motion, at the crests of the reinforced and unreinforced embankments, as well as at a depth of 60 cm directly underneath the embankments from the experiment and two different analyses. In all cases, the presence of reinforcement yields no significant difference in the acceleration at the embankment crest (the absolute value itself was different in both the tests and the analysis).

As for the behavior beneath the reinforced embankment, the test result and the result from the effective stress analysis coincide each other.

Table 4. Peak acceleration and amplification ratio to the input motion

At the crest of embankment

	With reinforcement	Without reinforcement
Shaking table test	257 / 1.49	257 / 1.49
Effective stress analysis	308 / 1.78	310 / 1.79
Total stress analysis	235 / 1.36	223 / 1.29

At 60cm depth underneath embankment

	With reinforcement	Without reinforcement
Shaking table test	252 / 1.46	327 / 1.89
Effective stress analysis	253 / 1.46	248 / 1.43
Total stress analysis	273 / 1.58	217 / 1.25

Peak acceleration (gal) / amplification ratio

(2) Excess pore water pressure in the ground

Figure 4 shows the time history of the excess pore water pressure ratio at a depth of 60 cm underneath the reinforced and unreinforced embankments. Note that the total stress analysis does not directly deal with excess pore water pressure. In the test, the excess pore water pressure ratio reached about 1.0 underneath the unreinforced embankment. Underneath the reinforced embankment, on the other hand, the peak excess pore water pressure ratio was around 0.5. In effective stress analysis, however, the value reaches 1.0 at around 6 seconds, regardless of whether the embankment is reinforced or not. It is not apparent for reason why this discrepancy occurred in the test. Based on the analytical result, there is little effect of the reinforcement on the reduction in the excess pore water pressure generation in the foundation ground. In the effective stress analysis, the excess pore water pressure increases immediately after the start of shaking. This is due to the overestimation of the amount of dilatancy of the initial loading.

(3) Subsidence of embankment

Figure 5 shows the time history of the subsidence at the crests of the reinforced and unreinforced embankments. Note that the result of the total stress analysis is only showed after shaking. In the case of the unreinforced embankment, test result and effective stress analytical result are in good agreement with regard to the amount of subsidence after shaking. The result of the total stress analysis predicts a much smaller value. The reinforced embankment settled one half of the unreinforced embankment in the test. In the effective stress analysis, however, the predicted values were the same for the unreinforced and reinforced embankments. This lesser amount of subsidence of the reinforced embankment in the test is thought to be due to a different tendency of pore water pressure generation in the ground underneath the embankment. Based on the analysis results, reinforcement is thought to have little effect on the subsidence of the embankment in this type of model.

Figure 6 shows a diagram of the deformation of the entire model after the shaking. The comparison between the test result and numerical analyses shows that both analytical methods simulate the deformation occurred during the test, such as the lateral flow in the ground underneath the embankments and so on.

(4) Embankment behavior

Figure 7 shows the time history of the ratio of the mean effective stress to the initial effective stress at the center of the reinforced and unreinforced embankments. As the foundation ground starts to liquefy after 6 seconds, the mean effective stress at

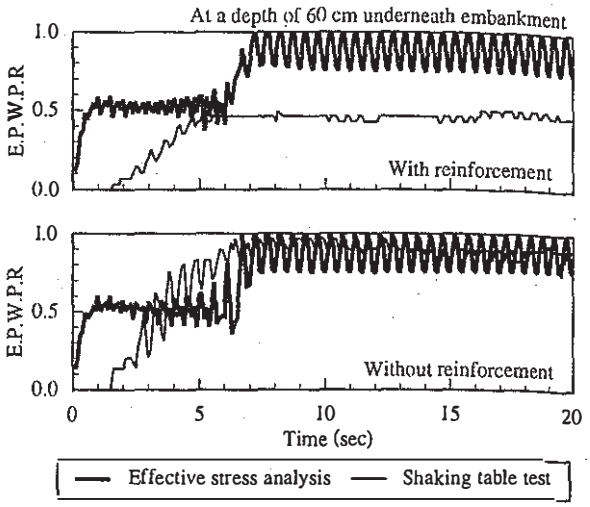

Figure 4. Time history of the excess pore water pressure ratio (Case 1)

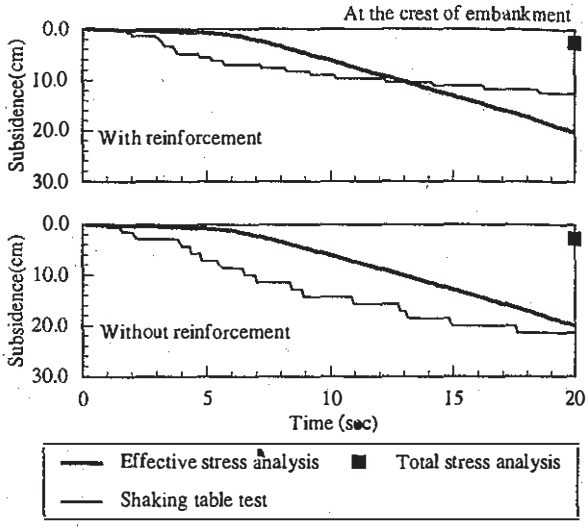

Figure 5. Time history of the subsidence (Case 1)

the center of the embankments decreases rapidly. In the unreinforced embankment, the mean effective stress falls straight down to zero, but in the reinforced embankment it stops at a value of around 40% of the initial value. It is evident that reinforcement can control the occurrence of tensile stress within the embankment. There is a possibility that cracks may occur in unreinforced embankments, in which tensile stress appears.

4.2 *Effect of the Type of Modeling (Analytical Case 2)*

According to the result in Section 4.1, there is little

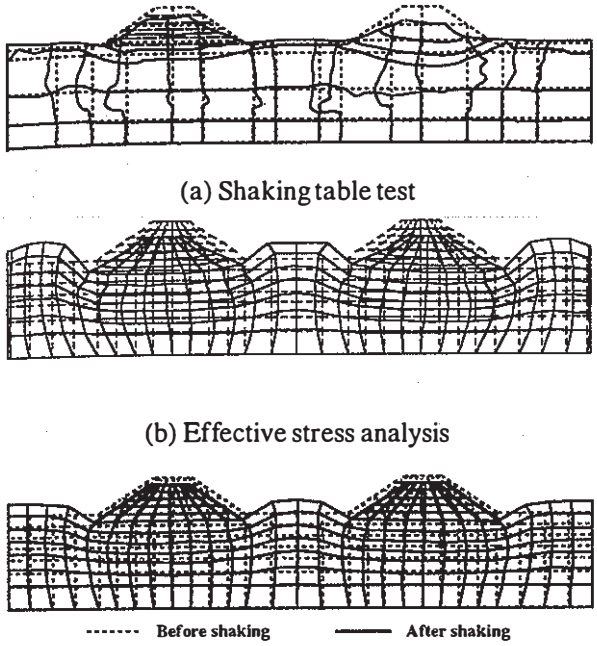

(a) Shaking table test

(b) Effective stress analysis

(c) Total stress analysis

Figure 6. Deformation of the entire model after the shaking (Case 1)

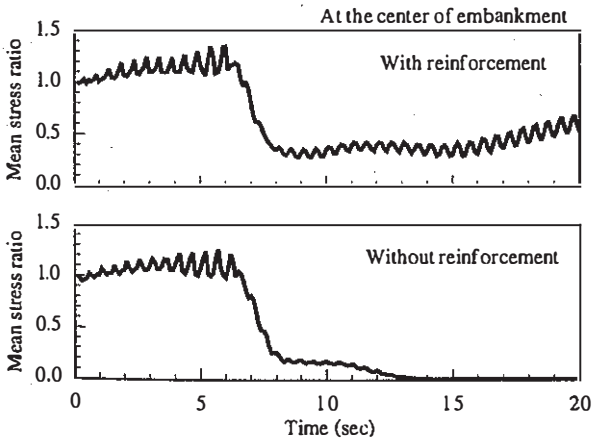

Figure 7. Time history of the mean effective stress ratio at the center of embankments (Case 1)

effect of reinforcement on embankment subsidence. In this section, we assume that the embankment has a higher rigidity using ideal reinforcement and model the embankments as elastic bodies.

(1) Acceleration response and excess pore water pressure in the ground

The tendencies in acceleration response and excess pore water pressure response is not different between Case 1 and Case 2. The time history of the excess pore water pressure ratio at a depth of 60 cm directly underneath the reinforced and unreinforced embankments is give in Figure 8. The tendency of pore water pressure generation underneath the reinforced embankment slightly differs from the analysis of Case 1. If the embankments are modeled as elastoplastic bodies (Figure 4), the excess pore water pressure increases dramatically for around 6 seconds. If the embankments are modeled as elastic bodies, the excess pore water pressure increases gradually to reach a value of 1.0. This is due to a difference in the deformation patterns of the embankments.

(2) Embankment subsidence and deformation

Figure 9 show the time history of the subsidence at the crests of the reinforced and unreinforced embankments. Based on the comparison between Figure 5 and Figure 9, the amount of subsidence in the reinforced embankment has been reduced by about 15%. It is thus believed that if embankments are perfectly reinforced into a single body, reinforcement can have an effect

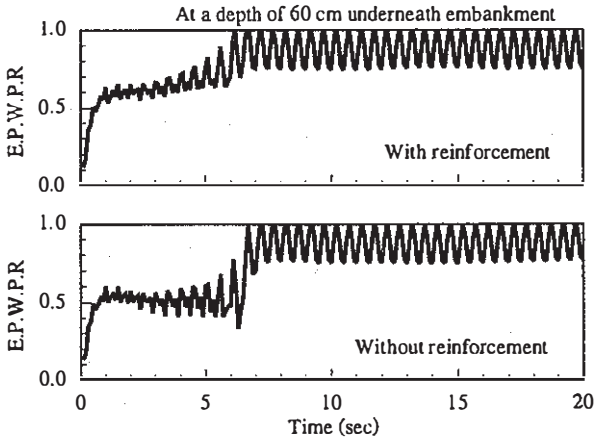

Figure 8. Time history of the excess pore water pressure ratio (Case 2)

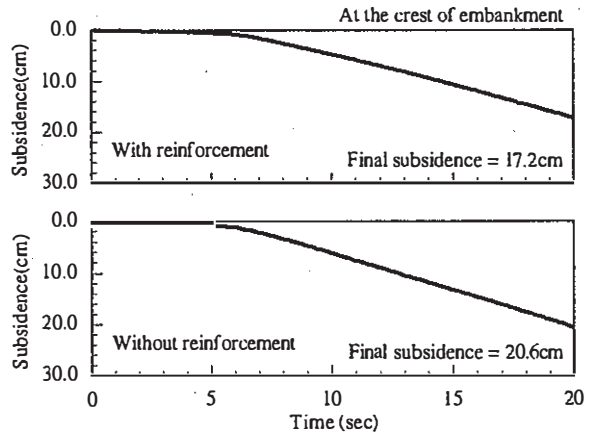

Figure 9. Time history of the subsidence(Case 2)

on the reduction in the embankment subsidence. A material of higher rigidity would have more profound effect on controlling subsidence.

5 CONCLUSIONS

Numerical simulations of liquefaction were conducted using the effective stress method, based on data from the shaking table test on embankments reinforced with non-woven fabric on liquefiable ground. The dynamic response of reinforced embankments on liquefiable ground and the effectiveness of reinforcement in controlling deformation were examined. As a result, the following were found:

- There is no difference in the acceleration response and excess pore water pressure response irrespective of the presence of reinforcement with non woven fabric.
- There is little effect of reinforcement with non-woven fabric on embankment subsidence.
- Although there is a possibility that reinforcement with non-woven fabric can control the occurrence of tensile stress within the embankments, further study is necessary to determine the reinforcement effect on the failure of the embankments themselves.
- It is thought that, if an embankment structure is perfectly reinforced into a single body by means of increasing the rigidity of the embankment using a reinforcement material with a higher rigidity than non-woven fabric, the reinforcement could have an effect on the reduction in the embankment subsidence.

ACKNOWLEDGMENTS

The shaking table tests of models used in the analytical simulations in this paper were carried out at the Public Works Research Institute of the Ministry of Construction, and the authors express their deep appreciation to Mr. Matsuo and Mr. Shimazu.

The total stress analysis was carried out by Fukken Co. Ltd. Consulting Engineers as part of their joint research project with PWRI, called "Joint Research for earthquake-resistant construction method for soft ground". We are deeply indebted to Dr. Fukuda, Dr. Tajiri, and Mr. Fujii, who were in charge of the analysis, for their help in determining analytical parameters. Also appreciated are the efforts of Mr. Shirakawa, student of Gifu University, in the preparation of the effective stress analysis.

REFERENCES

Fukuda, N. 1991: Utilization of geotextiles as reinforcement for soft ground, *GEO-COAST '91*, pp. 1150-1151.

Koseki, J. and Matsuo, O. 1995: Permanent deformation analysis of dynamic centrifugal model tests of embankments by earthquakes and its application example, *Civil Engineering Journal*, Public Works Research Institute, Vol. 37, No. 3, pp. 20-25 (in Japanese).

Oka, F. et al. 1994: A modified model for sand based on non-linear kinematic hardening rule, *Proc. of 28th Annual Meeting on SMFE*, pp. 486-490 (in Japanese).

Public Works Research Institute, Ministry of Construction 1989: Research of seismic subsidence of embankments and countermeasures, *Public Works Research Institute Report*, No. 2769, pp. 55-106 (in Japanese).

Public Works Research Institute, Ministry of Construction, et al. 1996: Joint research report (No. 3) for earthquake-resistant construction method for soft ground, *Joint Research Report* (in Japanese).

Shibata, T., Sato, T., Uzuoka, R., Oka, F., Yashima, A. and Kato, M. 1991: FEM-DEM coupled liquefaction analysis of a fluid saturated ground, *Proc. IACMAG 91*, Vol. 2, pp. 869-874.

Tateishi, A., Taguchi, Y., Oka, F. and Yashima, A 1995: A cyclic elastoplastic model for sand and its application under various stress conditions, *Proc. IS-Tokyo*, Vol. 1, pp. 399-404.

Tatsuoka, F., Muramatsu, M. and Sasaki, T. 1982: Cyclic undrained stress-strain behavior of dense sands by torsional simple shear test, *Soils and Foundations*, Vol. 22, No. 2, pp. 55-70.

Tatsuoka, F. and Yamauchi, H. 1986: A reinforcing method for steep clay slopes using a non-woven geotextile, *Geotextiles and Geomembranes 4*, pp. 241-268.

Tatsuoka, F., Tateyama, M. and Koseki, J. 1995: Performance of geogrid-reinforced soil retaining walls during the Great Hanshin-Awaji Earthquake of January 17, 1995, *Proc. IS-Tokyo*, Vol. 1 pp. 55-62.

White, D.M. and Holtz, R.D. 1994: Performance of geosynthetic-reinforced slopes and walls during the Northridge, California Earthquake of January 17, 1994